Materials Letters 410 (2026) 140253

Contents lists available at ScienceDirect

Materials Letters

journal homepage: www.elsevier.com/locate/matlet

Antiferroelectric phase dielectric relaxations in liquid crystal

Nidhi Pandey [a], Anoop Kumar Srivastava [b,*], Sudhanshu Pandey [a,e], Ramesh Manda [c], Rakesh Kumar [b], Dharmendra Singh [b], Ji-Hoon Lee [d]

[a] Faculty of Basic & Applied Sciences, Department of Physics, United University, Prayagraj, 211012, India
[b] Department of Applied Science and Humanities, Institute of Engineering and Technology, Dr. Rammanohar Lohia Avadh University, Ayodhya, 224001, India
[c] School of Physics, University of Hyderabad, Hyderabad, Telangana, 500046, India
[d] Division of Electronics Engineering, Jeonbuk National University, Jeonju, Jeonbuk, 54896, South Korea
[e] United Institute of Technology, Department of Applied Sciences, Naini, Prayagraj, 211010, India

ARTICLE INFO

Keywords:
Antiferroelectric liquid crystal
Polarization
Dielectric relaxation
Dielectric constant
Collective rotation

ABSTRACT

Antiferroelectric liquid crystal phase (SmC_A^*) is a unique type of chiral smectic phase characterized by an alternating alignment of molecular dipoles, where the polarization vectors of neighboring layers are oriented in opposite directions, leading to no overall spontaneous polarization unless an external field is applied. This behavior mirrors antiferroelectricity, akin to antiferromagnetism but in a soft matter context. In the SmC_A^* phase, two distinct dielectric relaxation modes are usually observed and reported in the literature: the high-frequency relaxation is attributed to molecular rotation, with molecules in antitilt pairs rotating in opposite directions around the cone. In contrast, the low-frequency dielectric mode is linked to molecular rotation in the same direction. Despite these observations, explaining the origin of the two modes through dielectric investigation remains challenging. To address this, simple, easy-to-understand explanations are proposed to elucidate the origin of the relaxation mode in the antiferroelectric phase of a liquid crystal.

1. Introduction

Electrostatic polarization is a fundamental phenomenon in physics and materials science, occurring when an external electric field causes a separation of charge within an insulating material, such as a dielectric. In such materials, the centres of positive and negative charges within atoms or molecules shift slightly in opposite directions, resulting in induced electric dipoles that align with or oppose to the applied field. Polarization affects the material's overall electric behavior, influencing key properties like the dielectric constant, which describes how much an electric field is reduced inside the material compared to vacuum. Polarization principles are integral to devices such as liquid crystal displays (LCDs), antennae, and medical imaging systems, where control over electrostatic behavior is essential. When polarization fails to follow the applied ac field, the dielectric relaxation occurs. The origin of dielectric relaxation plays a key role in advancing technologies such as actuators, transducers, and energy storage systems. It also helps researchers to connect the microscopic features of a material like crystal structure, impurities, defects and its overall electrical performance. [1]. It provides insight into polarization mechanisms, domain dynamics, and the coupling between the electric field and molecular reorientation [2–8]. In this paper, origin of two observed relaxation modes in antiferroelectric phase of liquid crystal material is elucidated through dielectric investigation.

2. Experimental

Measurements of relative dielectric permittivity (ε') and dielectric loss (ε″) were carried out using a Solartron 1260 impedance analyzer coupled with a 1296 dielectric interface, covering frequencies from 1.0 Hz to 1.0 MHz during the cooling cycle. Temperature regulation was achieved with an HS-1 unit controlled by an MK-1 system. The samples were fabricated as planar capacitors on indium tin oxide (ITO) coated glass substrates, with a 10 μm gap maintained using Mylar spacers. The ITO-bounded cell exhibited a sheet resistance of approximately 25 Ω/sheet. To calibrate the empty cell's capacitance, pure cyclohexane was used as a reference. Dielectric spectra were fitted using the following composite model [2,3].

* Corresponding author.
E-mail address: srivastava_anoop@rediffmail.com (A.K. Srivastava).

https://doi.org/10.1016/j.matlet.2026.140253
Received 10 January 2026; Received in revised form 6 February 2026; Accepted 9 February 2026
Available online 11 February 2026

$$\varepsilon^{*} = \varepsilon' - j\varepsilon'' = \varepsilon(\infty) + \sum_{i=1}^{2} \frac{(\Delta\varepsilon)_i}{1 + \left(j\,\frac{f}{f_{ri}}\right)^{(1-h_i)}} + \frac{A_1}{f^n} - j\frac{\sigma}{2\pi\varepsilon_0 f^k} - jAf^m \quad (1)$$

In this model, $\Delta\varepsilon_i$, h_i, f_{ri}, correspond respectively to the dielectric strength, distribution (broadening) exponent, and characteristic relaxation frequency of the *i*-th mode. The parameter $\varepsilon(\infty)$ represents the permittivity value approached at very high frequencies, while the term $\frac{A_1}{f^n}$ accounts for low-frequency polarization effects, such as Maxwell–Wagner interfacial polarization associated with the electrode capacitance. The fourth additive component in Eq. (1) represents energy dissipation due to dc conductivity. To address additional dielectric losses arising from the ITO coating's sheet resistance, stray capacitance and inductive effects in the leads, an extra term Af^m is analytically introduced. In this framework, n, m, A, k, and A_1 are fitting parameters, and ε_0 denotes the vacuum permittivity. The second term (dielectric relaxation term) of Eq. (1) was extracted by subtracting other terms of Eq. (1) by using fitting method. A Perkin-Elmer DSC-7 differential scanning calorimeter was employed to determine the transition temperature of the mixture.

3. Results and discussion

The W-132A mixture was formulated by blending of binary K128 and B2 multicomponent mixtures in a ratio of 18 and 82 wt% respectively. The compositions of K128 and B2 multicomponent mixtures are given below.

B2 composition

1. (*S*)-4-((octan-2-yloxy)carbonyl)phenyl 4′-(octyloxy)biphenyl-4-carboxylate of **18.52 wt%**
2. (*S*)-4-((octan-2-yloxy)carbonyl)phenyl 4′-(2-ethoxyethoxy)biphenyl-4-carboxylate of **13.99 wt%**
3. (*S*)-4-((octan-2-yloxy)carbonyl)phenyl 3-(decyloxy)benzoate of **20.00** wt%
4. (*S*)-4-((octan-2-yloxy)carbonyl)phenyl 3′-nonylbiphenyl-4-carboxylate of **38.22** wt%
5. (*S*)-octan-2-yl 4′-(4-(3-butoxypropoxy)benzoyloxy)biphenyl-4-carboxylate of **9.27**% wt%

K128 composition

1. (*S*)-octan-2-yl 4-(4-(3,3,4,4,5,5,6,6,7,7,8,8,9,9,10,10,10-heptadecafluorodecyloxy)benzoyloxy)benzoate of **12.90** wt%
2. (*S*)-octan-2-yl 4′-(4-(3,3,4,4,5,5,6,6,7,7,8,8,8-tridecafluorooctyloxy)benzoyloxy) biphenyl-4-carboxylate of **11.87** wt%
3. (*S*)-4-((octan-2-yloxy)carbonyl)phenyl 4′-(3,3,4,4,5,5,6,6,7,7,8,8,8-tridecafluorooctyloxy)biphenyl-4-carboxylate of **12.13** wt%
4. (*S*)-octan-2-yl 4-(4-(3,3,4,4,5,5,6,6,7,7,8,8,8-tridecafluorooctyloxy)benzoyloxy) benzoate of **38.80** wt%
5. (*S*)-4-((octan-2-yloxy)carbonyl)phenyl 3-fluoro-4′-(3,3,4,4,5,5,6,6,7,7,8,8,8-tridecafluorooctyloxy) biphenyl-4-carboxylate of **24.30** wt%

Using DSC, the phase sequence of I(103–85 °C) Smectic A* (59–53 °C) Smectic C*(48 °C) Smectic C_A* (< 0 °C) was observed during cooling cycle. It is important to mention here that both (B2 and K128) show a phase sequence of SmC*-SmA*-I and none of them show SmC_A* phase. The SmC_A* phase is induced with carefully adjusted component ratios. The dielectric relaxation behavior is analyzed by using Eq. (1). Fig. 1 explain that how the dielectric relaxation modes are extracted by using Eq. (1). Initially, the experimental dielectric permittivity and dielectric loss curves were fitted using an Eq. 1. Thereafter, we extracted or resolved the second term (dielectric relaxation term) by subtracting the other terms from experimental data. The frequency-dependent response of extracted ε' and ε'' for smectic A* (SmA*) and smectic C* (SmC*) phases at different temperatures are illustrated in Fig. 2. A single relaxation process was detected in both the SmA* and SmC* phases. This relaxation is identified as the soft mode in the SmA* phase and as the Goldstone mode in the SmC* phase. Details for these modes are reported in detail in ref. [2, 3].

The extracted ε' and ε'' curves for SmC_A* at different temperatures are shown in Fig. 3. Two absorption peaks (R_H and R_L) were observed in

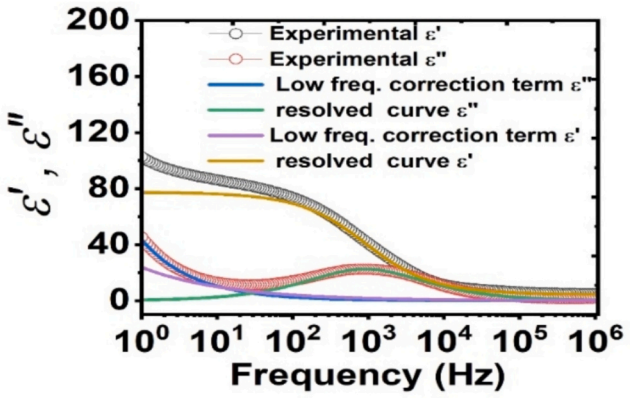

Fig. 1. SmC* phase dielectric response at 49.3 °C. Purple circles show experimental ε' data; the solid purple line indicates the best fit using Eq. (1). Red circles depict experimental ε″ data, and the continuous red curve representing the corresponding fit. A violet curve illustrates the low-frequency correction applied to ε', while the mud-brown line displays ε' after this correction has been subtracted. A blue curve shows the low-frequency correction for ε″, and the green line represents ε″ with the correction removed. (For interpretation of the references to colour in this figure legend, the reader is referred to the web version of this article.)

SmC_A* phase and their relaxation frequency were separated by two decades of frequency. Many authors have proposed that high frequency relaxation modes are associated to soft mode [4,9]. Some previous studies have attributed this mode to distortions in the antiferroelectric ordering [10,11], while the low-frequency relaxation has been associated with non-collective molecular reorientation about the short axis [9–11]. In 1995, Baviidas et al. and later in 1998, Panarin et al. attributed R_H as collective molecular rotation around the tilt cone, where molecules in antitilt pairs oscillate in opposite directions (antiphase mode) and R_L was linked to rotation in which molecules in antitilt pairs rotate in the same direction around the cone (in-phase mode) [13,14]. Their explanation was quite reasonable, satisfactory and acceptable till date but it was little intricate. Herein, both modes are explained by considering the only ε' values for both the modes. The ε' of the materials can be expressed as

$$\varepsilon' = \frac{E_0}{E}, \quad (2)$$

where E_0 is and an external electric field and E is the net electric field inside the dielectric. In case of high ε', the polarization will be in opposite direction. Therefore, the internal electric field (E_{in}) developed in the dielectric will oppose E_0. The net electric field E ($E = E_0 - E_{in}$) developed inside the dielectric and will be less than E_0. Hence, according to Eq. (2), the value of ε' will be greater than one. Just in case, if polarizations are in the same direction as the external field, it would lead to an increase in the net electric field ($E = E_0 + E_{in}$), inside the dielectric. In such a case, E would be greater than E_0. Therefore, as per Eq. (2), the ε' would be less than one.

According to Fig. 3, the ε' for high frequency relaxation mode is greater than one whereas in case of low frequency mode, it is less than one. Therefore, it is clear from above made analysis that in case of R_H mode the polarization will be in opposite direction whereas in case of R_L mode the polarization is in same direction i.e. in case of R_H mode the molecules are rotating in opposite direction around the cone in their antitilt position whereas in case of R_L mode they are rotating in the same direction. We also cross checked our proposed logic for other antiferroelectric liquid crystal named as MOPB(*H*)PBC [3]. The dielectric constant observed for low frequency relaxation mode in antiferroelectric phase was less than one (0.24 at 1 kHz) whereas for high frequency mode, it was greater than one (1.12 at 1 kHz).

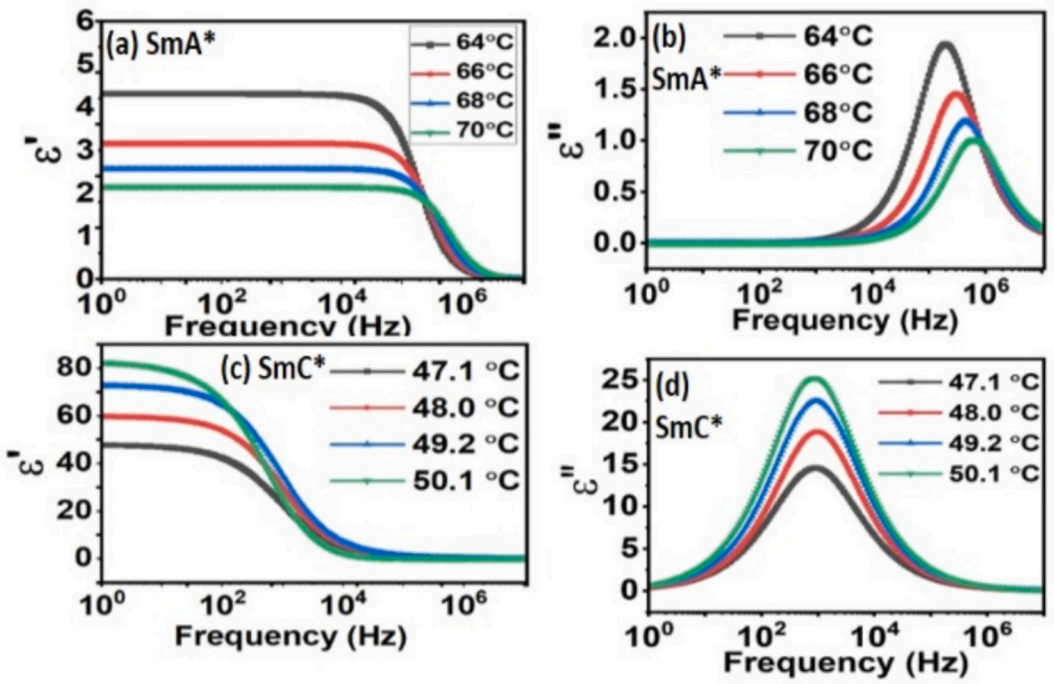

Fig. 2. Variation of (a,c) dielectric constant (ε') and (b,d) loss (ε") as a function of frequency recorded at multiple temperature settings for SmA* phase and SmC* phase respectively.

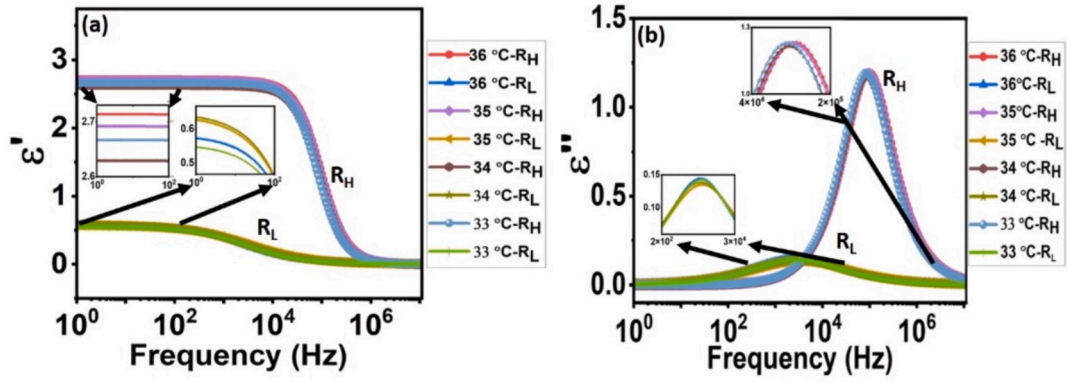

Fig. 3. Variation of (a) dielectric constant (ε') and (b) loss (ε") as a function of frequency for SmC_A* phase as a function of frequency, recorded at multiple temperature settings.

4. Conclusions

The origin of relaxation modes in antiferroelectric phase of liquid crystal is explained via dielectric analysis. Two relaxation modes in ~50 kHz (R_H mode) and ~ 500 Hz (R_L mode) region were observed in antiferroelectric phase of liquid crystal. The origin of these modes is explained by corelating the value of relative dielectric permittivity and direction of polarization of molecules with respect to the applied electric field. The R_H mode is assigned as antiphase rotation of molecules because of its relative dielectric permittivity greater than 1 whereas the R_L mode is assigned as in-phase motion of molecules due to its relative dielectric permittivity lower than 1.

CRediT authorship contribution statement

Nidhi Pandey: Writing – review & editing, Investigation, Formal analysis. **Anoop Kumar Srivastava:** Writing – review & editing, Writing – original draft, Supervision, Resources, Methodology, Investigation, Data curation, Conceptualization. **Sudhanshu Pandey:** Formal analysis. **Ramesh Manda:** Formal analysis. **Rakesh Kumar:** Formal analysis. **Dharmendra Singh:** Writing – review & editing, Formal analysis. **Ji-Hoon Lee:** Writing – review & editing, Formal analysis.

Funding

No funding was received"

Declaration of competing interest

The authors declare that we have no known conflict of interest, competing financial interests or personal relationships that could have appeared to influence the work reported in this paper.

Appendix A. Supplementary data

Supplementary data to this article can be found online at https://doi.

org/10.1016/j.matlet.2026.140253.

Data availability

Data will be made available on request.

References

[1] J.H. Ryu, J.W. Yu, T.J. Yoon, W.B. Lee, J. Mol. Liq. 397 (2024) 124054.
[2] A.K. Srivastava, V.K. Agrawal, R. Dabrowski, J.M. Otón, R. Dhar, J. Appl. Phys. 98 (2005) 013543.
[3] A.K. Srivastava, V.K. Agrawal, R. Dhar, S.H. Lee, R. Dabrowski, Liq. Cryt. 35 (2008) 1101–1108.
[4] T. Fujikawa, H. Orihara, Y. Ishibashi, Y. Yamada, N. Yamamoto, K. Mori, K. Nakamura, Y. Suzuki, Takashi Hagiwara, Ichiro Kawamura, Jpn. J. Appl. Phys. 30 (1991) 2826–2831.
[5] P. Perkowski, M. Urbańska, Materials 17 (2024) 3335.
[6] M. Buivydas, F. Gouda, G. Andersson, S.T. Lagerwall, B. Stebler, J. Bömelburg, G. Heppke, Liq. Cryst. 23 (1997) 723–739.
[7] M. Marzec, A. Mikułko, S. Wróbel, W. Haase, R. Dąbrowski, Mol. Cryst. Liq. Cryst. 436 (2005) 169–180.
[8] A. Mishra, R. Dąbrowski, R. Dhar, J. Mol. Liq. 249 (2018) 106–109.
[9] H. Moritake, Y. Uchiyama, K. Myojin, M. Ozaki, Ferroelectrics 147 (1993) 53–66.
[10] H. Uehara, Y. Hanakai, J. Hatano, S. Satio, K. Murashiro, Jpn. J. Appl. Phys. 34 (1995) 5424–5428.
[11] K. Hiraoka, H. Takezoe, A. Fukada, Ferroelectrics 147 (1993) 13–25.
[13] M. Buivydas, F. Gouda, S.T. Lagerwall, B. Stebler, Liq. Cryst. 18 (1995) 879.
[14] Y.P. Panarin, O. Kalinvoskaya, J.K. Vij, Appl. Phys. Lett. 72 (1998) 1667–1669.

Further reading

[12] J. Hatano, Y. Hanakai, H. Furue, H. Uehara, S. Saito, K. Murashiro, Jpn. J. Appl. Phys. 33 (1994) 5498.